Cell Cycle

ISSN: 1538-4101 (Print) 1551-4005 (Online) Journal homepage: http://www.tandfonline.com/loi/kccy20

Molecular Basis for the Inhibition of p53 by Mdmx

Grzegorz M. Popowicz, Anna Czarna, Ulli Rothweiler, Aleksandra Szwagierczak, Marcin Krajewski, Lutz Weber & Tad A. Holak

To cite this article: Grzegorz M. Popowicz, Anna Czarna, Ulli Rothweiler, Aleksandra Szwagierczak, Marcin Krajewski, Lutz Weber & Tad A. Holak (2007) Molecular Basis for the Inhibition of p53 by Mdmx, Cell Cycle, 6:19, 2386-2392, DOI: 10.4161/cc.6.19.4740

To link to this article: https://doi.org/10.4161/cc.6.19.4740

Published online: 02 Oct 2007.

[Cell Cycle 6:19, 2386-2392, 1 October 2007]; ©2007 Landes Bioscience

Report

Molecular Basis for the Inhibition of p53 by Mdmx

Grzegorz M. Popowicz[1]
Anna Czarna[1]
Ulli Rothweiler[1]
Aleksandra Szwagierczak[1]
Marcin Krajewski[1]
Lutz Weber[2]
Tad A. Holak[1]*

[1]Max Planck Institute for Biochemistry; Martinsried, Germany

[2]NexusPharma Incorporated; Langhorne, Pennsylvania

*Correspondence to: Tad A. Holak; Max Planck Institute for Biochemistry; Am Klopferspitz 18a; Martinsried 82152 Germany; Tel.: +49.89.8578.2673; Fax: +49.89.8578.3777; Email: holak@biochem.mpg.de

Original manuscript submitted: 07/08/07
Manuscript accepted: 07/12/07

Previously published online as a *Cell Cycle* E-publication:
http://www.landesbioscience.com/journals/cc/article/4740

KEY WORDS

Mdmx, Mdm4, p53, cancer, nutlin, structure

ACKNOWLEDGEMENTS

We thank Reinhard Koester for the zebrafish DNA.

ACCESSION CODES

Protein Data Bank. Coordinates have been deposited with accession codes 2Z5S and 2Z5T.

NOTE

Supplementary materials can be found at:
http://www.landesbioscience.com/supplement/PopowiczCC6-19-Suppl.pdf

ABSTRACT

The oncoprotein Mdm2, and the recently intensely studied, homologues protein Mdmx, are principal negative regulators of the p53 tumor suppressor. The mechanisms by which they regulate the stability and activity of p53 are not fully established. We have determined the crystal structure of the N-terminal domain of Mdmx bound to a 15-residue p53 peptide. The structure reveals that although the principle features of the Mdm2-p53 interaction are preserved in the Mdmx-p53 complex, the Mdmx hydrophobic cleft on which the p53 peptide binds is significantly altered: a part of the cleft is blocked by sidechains of Met and Tyr of the p53-binding pocket of Mdmx. Thus specific inhibitors of Mdm2-p53 would not be optimal for binding to Mdmx. Our binding assays show indeed that nutlins, the newly discovered, potent antagonists of the Mdm2-p53 interaction, are not capable to efficiently disrupt the Mdmx-p53 interaction. To achieve full activation of p53 in tumor cells, compounds that are specific for Mdmx are necessary to complement the Mdm2 specific binders.

INTRODUCTION

Loss of p53 function through mutations is involved in 50% of human cancer; the remainder retains wild-type p53 but the p53 pathway is inactivated through the interaction with the Mdm2 and Mdmx proteins.[1-8] Mdm2, the first to gain the status of a principal cellular antagonist of p53, acts as an ubiquitin ligase, promoting ubiquitination of p53 followed by degradation in proteasome.[9,10] As Mdm2 gene is regulated by p53 pathway, the proper level of p53 is maintained by autoregulatory feedback.[11,12] Mdm2 interacts primarily through its 100 residue N-terminal domain with the N-terminal transactivation domain of p53 (see refs. 13–18).

Mdmx has only recently emerged as a critical, independent regulator of p53 activation.[2,3,7,8,19-27] Although Mdmx is highly homologous to Mdm2 (Suppl. Fig. 1), it does not possess ubiquitin ligase capability[20,28] and its expression level is not p53 dependent. It was shown that Mdmx could inhibit p53 transcriptional activity even stronger than Mdm2 (see refs. 2, 3, 19, 21, 24 and 27); and both proteins cooperate in inactivation of p53 (see refs. 2 ,3, 7, 8 and 27). The mechanism of the Mdm2/Mdmx regulation of p53 is however not clearly understood; in particular, the contributions of Mdm2 versus Mdmx to the regulation of p53 stability and activity is unclear, although the very recent model for p53 regulation by Mdm2 and Mdmx seems to remove many controversial propositions.[2,24]

The rescue of the impaired p53 function by disrupting the Mdm2-p53 interaction offers new avenues for anticancer therapeutics[4,5,29-33] and several lead compounds have recently been reported to inhibit the p53-Mdm2 interaction.[4,5,32,33] The first and still the best-documented drug-like compounds developed are cis-imidazoline derivatives called nutlins.[5,32] Nutlin-3 is a selective and potent inhibitor of the p53-Mdm2 interaction, which induces apoptosis in p53 wild-type cells and shows in vivo efficacy in mice xenograft models. For Mdmx, several recent studies concluded that nutlin-3 does not disrupt Mdmx-p53 complexes[22,25,26] whereas one most recent report[23] provides evidence that the potency of nutlin-3 is sufficient to disrupt the Mdmx-p53 interaction and to efficiently kill retinoblastoma cancer cells.[3,23] These authors furthermore found that subconjunctival administration of nutlin-3 with topotecan, a drug that induces a p53 response through DNA damage, could achieve synergistic tumor cell killing in patients, without causing the side effects associated with prolonged systemic exposure.[3,23]

We present here the structure of Mdmx bound to the 15-residue peptide from the transactivation domain of p53. The structure of Mdmx/p53 reveals the mechanism of p53 inhibition by Mdmx and predicts that specific inhibitors of Mdm2-p53 would not be optimal for binding to Mdmx. To test this prediction, we examined the capablility of nutlin-3 to dissociate the Mdmx-p53 complex. We show that the potency of nutlin-3 is low; at high concentrations, only a small fraction of p53 can be recovered from the p53/Mdmx complex, whereas a 100% p53 recovery is observed in the nultin/Mdm2/p53 system.

MATERIALS AND METHODS

Protein expression and purification. The human Mdmx (Hdmx) domain between residues 1–134, Hdmx mutants M53V and Y99T, the p53-binding domains of zebrafish Mdmx (residues 15–129) and the "human mimic" Mdmx (residues 15–129, mutations L46V and V95L) were obtained from an *E. coli* BL21(DE3) RIL expression system using the pET-46Ek/LIC vector. Cells were grown at 37°C and induced with 1 mM IPTG at an OD_{600nm} of 0.7. The proteins were expressed for 12 h at 20°C. The proteins were first purified under native condition using Ni-NT Agarose (Qiagen) and finally by HiLoad 16/60 Superdex75 gel filtration (Pharmacia). The uniformly ^{15}N isotopically enriched protein samples were prepared by growing the bacteria in minimal media containing $^{15}NH_4Cl$. The recombinant human p53 protein (residues 1–310) was overexpressed at 37°C overnight in *E. coli* BL21(DE3) RIL using the pET-46Ek/LIC vector. The protein was purified under denaturing conditions using a Ni-NTA (Qiagen) column, refolded, and further purified using a Heparin Sepharose 6 Fast Flow (Amersham) column. Final purification was carried out via a HiLoad 16/60 Superdex75 gel filtration column.

The recombinant human p53 protein (residues 1–73) was overexpressed at 37°C for 3 h in *E. coli* BL21 using a pGEX vector. The protein was purified under native conditions via GST-Sepharose FF (Pharmacia). Final purification was carried out via a HiLoad 16/60 Superdex75 gel filtration column. Human Mdm2s (Hdm2s), residues 1–118 and 1–125, were expressed using the pET46-Ek/LIC vector and purified from inclusion bodies as previously (described in ref. 34). The p53 peptides were chemically synthesized and were purified by reversed phase chromatography. The p53 peptide 1, comprising residues 15 to 29 of human p53, contained the sequence: SQETFSDLWKLLPEN; peptide 2 had the sequence: RFMDYWEGL; and the zebrafish p53 peptide Z, comprising residues 5 to 20, has the sequence: DSQEFAELWEKNLIIQ.

X-ray crystallography. The protein buffer used for crystallization contained 5 mM Tris/HCl pH 8.0 and 50 mM NaCl. Crystallization of the protein was carried out with the sitting drop vapor diffusion method. Zebrafish Mdmx crystallized in the form of very thin plates from a crystallization solution containing 30% PEG 300, 0.1 M MES pH 6.5. They appeared in several days and grew to a final size of ca. 0.3 x 0.1 x 0.01 mm. Crystals were directly plunged frozen. The crystals belong to the space group $P2_1$ and contained three complexes per an asymmetric unit. An acceptable quality dataset up to 2.3 Å was collected on the MPG/GBF beamline BW6 at DESY, Hamburg, Germany. The collected data were integrated, scaled and merged by XDS and XSCALE programs.[35] The structures were determined by molecular replacement using the Molrep program from the CCP4 suite.[36] The structure of the Hdm2 taken from the PDB entry 1T4F (see ref. 33) was used as a probe. The initial R-factor of the model was 0.46. The models were then refined by Refmac5 (see ref. 38) and rebuilt by XtalViev/Xfit (see ref. 37) and by a subsequent Refmac5 refinement. Water molecules were added by Arp/warp (see ref. 38). The final R crystallographic factor was 0.21 and R_{free} 0.27 and 0.25/0.31 for the "human-mimicking" and native structures, respectively. Most of the Mdmx models had clear interpretable electron density between Arg15 and Leu106, with M chain having barely interpretable electron density from lysine and isoleucine from the enterokinase cleavage site preceding Arg15 of Mdmx. Certain solvent exposed side-chains without clear electron density were omitted in the model. Data collection and refinement statistics are summarized in Table 1.

NMR methods. All NMR spectra were acquired at 300 K on a Bruker DRX 600 MHz spectrometer equipped with a cryoprobe. Typically, NMR samples contained up to 0.26 mM of protein in 50 mM KH_2PO_4, 50 mMNa_2HPO_4, 150 mM NaCl, 5 mM DTT, pH 7.4. For ^1H-^{15}N HSQC spectra, a total of 1024 complex points in t_2 and 128 t_1 increments were acquired. Water suppression was carried out using the WATERGATE sequence. NMR data were processed using the Bruker program Xwin-NMR version 3.5.

NMR ligand binding experiments were carried out in an analogous way to those (as previously described in refs. 34, 39 and 40) 500 µl of the protein sample containing 10% D_2O, at a concentration of about 0.2 mM, and a 20 mM stock solution of nutin-3 (purchased from Cayman Chemical, MI) in DMSO-*d*6 were used in all of the experiments. p53 peptides were dissolved in PBS. The maximum concentration of DMSO at the end of titration experiments was about 2–3%, except for the titration of Hdmx/p53 with nutlin-3, where it was 10% (to ensure that nutlin-3 was dissolved at its 50-fold excess molar concentration relative to the protein). The pH was maintained constant during the entire titration. As controls, to check the effect of DMSO on the proteins, we titrated the protein complex and proteins with DMSO up 10%. We found no significant changes in terms of chemical shifts, precipitation, or denaturation of the proteins for DMSO concentrations used in the compound titrations. We thus conclude that the DMSO effect on the proteins while titrating with different compounds can be neglected.

Isothermal titration calorimetry (ITC). The binding of different p53 constructs to Hdm2 (residues 1–118), Hdmx (residues 1–134), and Mdmx (residues 15–129) was measured by isothermal titration calorimetry using a VP-ITC MicroCalorimeter (MicroCal, Northampton, MA). The protein concentration in the reservoir solution was around 0.02–0.03 mM, the concentration of the titrant was around 0.2–0.3 mM. Measurements were carried out in PBS, 2 mM TCEP, pH 7.4). All steps of the data analysis were performed using ORIGIN(V5.0) software provided by the manufacturer.

RESULTS

Structure of the Mdmx-p53 complex. The X-ray structure of a complex between human p53 (residues 15-29) and a variant of zebrafish Mdmx (residues 15–129), in which the p53 binding site has been mutated to that of human Mdmx (Hdmx), was solved by molecular replacement using the structure of human Mdm2 (Hdm2) 1T4F (see ref. 33) as a model. We also solved the structure of the wild-type zebrafish Mdmx (residues 15–129) bound to human p53

Table 1 **Data collection and refinement statistics**

Data Collection	**Native**	**Human-Mimic**
Space group	$P2_1$	$P2_1$
Cell constants (Å)	a=80.52	a=81.08
	b=30.44	b=30.54
	c=100.85	c=101.1
	β=102.47	β=102.94
Resolution range (Å)	30-2.3	30-2.3
Wavelength (Å)	1.05	1.05
Observed reflections	102529	93820
Unique reflections	21546	23555
Whole resolution range:		
Completeness (%)	91.6	93.2
R_{merge}	13.5	9.32
I/σ(I)	8.42	14.0
Last resolution shell		
Resolution range (Å)	2.3-2.4	2.3-2.4
Completeness (%)	82.0	96.3
R_{merge}	30.0	25
I/σ(I)	4.0	5.25
Refinement		
No. of reflections	20724	18354
Resolution (Å)	20-2.3	20-2.4
R-factor (%)	24.7	21.0
R_{free} (%)	31.0	26.4
Average B ($Å^2$)	26.25	21.14
R.m.s bond lenght (Å)	0.009	0.009
R.m.s. angles (°)	1.426	1.2
Content of asymmetric unit		
RMSD of monomers (Å)	0.47	0.5
No. of complexes	3	3
No. of protein residues/atoms	296/2377	307/2490
No. of solvent atoms	147	355

(residues 15 to 29) (Table 1). The structures are closely similar (rmsd for the mainchain superposition is 0.39 Å) and we will concentrate below on the structure of the human-mimic Mdmx. Crystallization of the N-terminal domain of Hdmx produced crystals that were not suitable for structural analysis, whereas zebrafish Mdmx crystals diffracted up to 2.2–2.3 Å. Sequence alignment shows that the wild-type zebrafish Mdmx is highly homologues both to Hdmx (identity 48.8% for the full-length proteins, and identity 66%, similarity 85% within the 95 residues included in the structures) and to Hdm2 (identities 33.5%, 50.0%, similarity 74%, respectively) (Suppl. Fig. 1). Considering the residues important for the p53 binding in these proteins, the zebrafish Mdmx is closer to human Mdmx than to human Mdm2. The amino acid sequence of the native zebrafish Mdmx differs from that of Hdmx only by Leu46 and Val95 in the p53 binding region and thus these residues were mutated to Val46 and Leu95 to achieve the human-featured p53 binding site.

The major difference between amino acid sequences of the first 100 residues of Mdmx and Hdm2 is at a stretch of the Hdm2 residues His96-Arg97-Lys98-Ile98, which are replaced by Pro95-Ser96-Pro97-Leu98 and Pro92-Ser93-Pro94-Val95 in Hdmx and zebrafish Mdmx, respectively. The affinities of zebrafish Mdmx´s for the largest fragment of p53 (residues 1–310) and for nutlin-3 are analogous to those of Hdmx (Table 2). Thus we have concluded that zebrafish Mdmx should be an excellent model for its human counterpart.

The overall fold of zebrafish Mdmx is similar to that of Hdm2 (rmsd for the heavy atoms superposition between residues 25–109 of Hdm2 and residues 20–106 of zebrafish Mdmx is 1.28 Å) (Fig. 1A). The fold preserves the principal elements of the structure of Hdm2: a structural repetition into two portions of about 40 residues long, β1α1β2α2 and β1'α1'β2'α2', that are related by an approximate dyad axis of symmetry,[16] and a hydrophobic cleft on one side of the structure formed by the repeat packing across their hydrophobic sides. The leading difference is located in helix α2'. This helix is moved by 2.5 Å in zebrafish Mdmx towards its C-terminus compared to Hdm2. It also starts later, all because of the Pro92-Ser93-Pro94 sequence; however the changes in α2´ start already at the zebrafish Mdmx Asn91 (Hdm2, Glu95) and the α2´ helices of zebrafish Mdmx and Hdm2 get successively out of the register to each other until Leu103 (Hdm2: Leu107), without large single differences in ϕ,ψ angles (Fig. 1B). It is worth mentioning here that the ϕ,ψ angles of the Pro92-Ser93-Pro94 sequence are still in the α-helical range (Suppl. Fig. 2). The binding cleft of zebrafish Mdmx is smaller than that of Hdm2 (Fig. 2). This is because the sidechain of Tyr96 protrudes into the binding pocket, making it shallower (despite that Cα is moved by 1 Å to the outside of the cleft, towards helix α1', e.g., away from the center of the p53-binding pocket). The position of the aromatic ring of Tyr96 is identical in all Mdmx molecules present in our structures, but different compared to that of the corresponding Hdm2 Tyr100 seen in all resolved structures of Hdm2 (Fig. 1A and B). In those structures Tyr100 participates in a rim around the p53-binding site; which is primarily made up by the sidechain of the Hdm2 His96. Zebrafish Mdmx has Pro92 (Pro97 in Hdmx) at this position; thus the rim of the Mdm2 structure is effectively absent in zebrafish Mdmx. This makes the binding cleft of Mdmx shallower on the side of α2'. When the structure is viewed in the standard orientation of (Fig. 1A), the apex of the p53-binding cleft is further blocked from the opposite side by the sidechain of Met50 of helix α2 of zebrafish Mdmx (Met53 in Hdmx). The Met50 sidechain points into the p53-binding pocket (this is the same orientation as the corresponding Leu46 of Hdm2 (Ile50 in *Xenopus laevis* Mdm2) but the larger Met50 sidechain makes the p53-binding cleft smaller (Figs. 1A and 2). Other distinct differences in amino acid sequences between Mdmx and Hdm2 are the Hdm2 residues 86 and 104. There is Leu82 (Leu85 in Hdmx) instead of Phe86 at the bottom of binding site in zebrafish Mdmx and no Tyr104 - instead we have Lys100 (Arg103 in Hdmx). These substitutions however have small effects on the shape of the p53-binding cleft; for example, the aromatic ring of the Hdm2 Tyr104 is filled with the sidechain of Leu17 in Mmdx.

Determinants of the binding of p53 to Hdm2 found in the p53-Hdm2 interaction remain mostly intact for the p53-Mdmx binding. The primary contacts to Mdmx are made by hydrophobic Phe19, Trp23, and Leu26 of human p53 that form together an interface that is complementary to and fills up a hydrophobic pocket of zebrafish Mdmx (Fig. 1B). In the p53 peptide, the sidechains of Phe19 and Trp23, which insert deep into the zebrafish Mdmx cleft,

Table 2 **ITC and NMR titration data for various peptide/small-molecule binding partners of Hdm2, Hdmx and zebrafish Mdmx**

Binding Partner	Hdm2	Hdmx	Zebrafish Mdmx	Human-Mimic Mdmx
p53 (res. 1-310)	0.77 ± 0.07	0.48 ± 0.05	0.35 ± 0.03	0.45 ± 0.04
p53 (res. 1-310)	0.39 ± 0.20[a]			
GST-p53 (res. 1-73)	0.50 ± 0.05	0.13 ± 0.03	0.40 ± 0.06	
GST-p53 (res. 1-73)		0.10 ± 0.01[b]		
GST-p53 (res. 1-73)		0.29 ± 0.05[c]		
GST-p53 (res. 1-73)		1.51 ± 0.3[d]		
p53 peptide 1	0.60 ± 0.07	0.21 ± 0.05	2.20 ± 0.30	2.40 ± 0.40
p53 peptide 2	0.45 ± 0.05	35 ± 20	40 ± 30	-
p53 peptide Z	1.22 ± 0.2	3.6 ± 0.4	0.67 ± 0.05	1.33 ± 0.2
Nutlin-3	0.70 ± 0.08	25 ± 18	28 ± 20	25 ± 20
Nutlin-3		5 ± 2[c]		
Nutlin-3		200 ± 20[d]		
NXN-6	2 ± 1	500 ± 120	-	-
NXN-7	4 ± 2	-	-	-

K_D values in μM. K_D values were determined by NMR in case of fast exchange/weak binders (K_D´s > 8 μM). Peptide 1: human p53 sequence S_{15}QETFSDLWKLLPEN$_{29}$; peptide 2: RFMDYWEGL (refs. 41–43); the zebrafish p53 peptide Z, sequence: D_5SQEFAELWEKNLIIQ$_{20}$. Entries: -, not measured; [a]Hdm2 (residues 1–125); [b]Hdmx (res. 1–112); [c]Hdmx(M53V; [d]Hdmx(Y99T).

are seen in the same positions in both Hdm2 and zebrafish Mdmx structures. However, the segment of the p53 peptide starting at Leu25, e.g., Leu25-Leu26-Pro27, is ca 1.7 Å shifted to the outside compared to that in Hdm2 (Fig. 1B).

Nutlin-3, NXN-6 and NXN-7 are weak competitors of p53 in binding to Mdmx. The affinities of Mdmx versus Hdm2 (human Mdm2) for p53 are similar, in the range of 0.1–2 μM for the p53 protein fragments and the p53 peptide 1 (Table 2) and are in agreement with the results of Laurie et al.[23] for the p53 peptide/Hdmx and close to the K_D obtained for the N-terminal domain of Hdm2/peptide 1 (K_D=0.6 μM, see ref. 16). Interestingly, the same experiments performed for a 9mer of the "optimized" p53 peptide,[41-43] used for crystallization of Hdm2 by Grasberger et al.,[33] showed weak binding and fast exchange in NMR between bound and unbound states of Mdmx (Table 2 and data not shown). Our K_D data is broadly in agreement with the results of Böttger et al.,[44] who tested a number of different p53 peptides for binding to Mdmx and Mdm2.

To check whether nutlin-3 is capable to compete with p53 for binding to Mdmx's, we have monitored the influence of nutlin-3 on NMR spectra of a purified complex of the N-terminal domain of Hdmx and GST-p53 (residues 1–73) and compared these results with the corresponding Hdm2/p53 spectra. Top traces in all panels in (Fig. 4) show 1D proton NMR spectra of the NH side chains of Trp residues of the free, Hdm2/Hdmx unbound p53. Because of a highly flexible nature of the N-terminal domain of p53, the side chains of Trp23 and Trp53 give rise to sharp lines.[17,39,45,46] On forming the complex with Hdm2 or Hdmx, the signal of Trp23 disappears (Fig. 4, middle traces in all panels). This is because Trp23, together with the p53 residues 17 to 26, comprise the primary binding site for Hdm2 and Hdmx. Upon binding, these residues participate in well-defined structures of large p53-Hdm2, p53-Hdmx complexes, whereas Trp53 is still not structured when p53 is bound to Hdm2 or Hdmx (see ref. 39). The observed $1/T_2$ transverse relaxation rate of the bound Trp23 in the complexes increases thus significantly and broadening of NMR resonances results in the disappearance of this signal in the spectra.[39] Nutlin-3 was then added to the Hdm2/p53

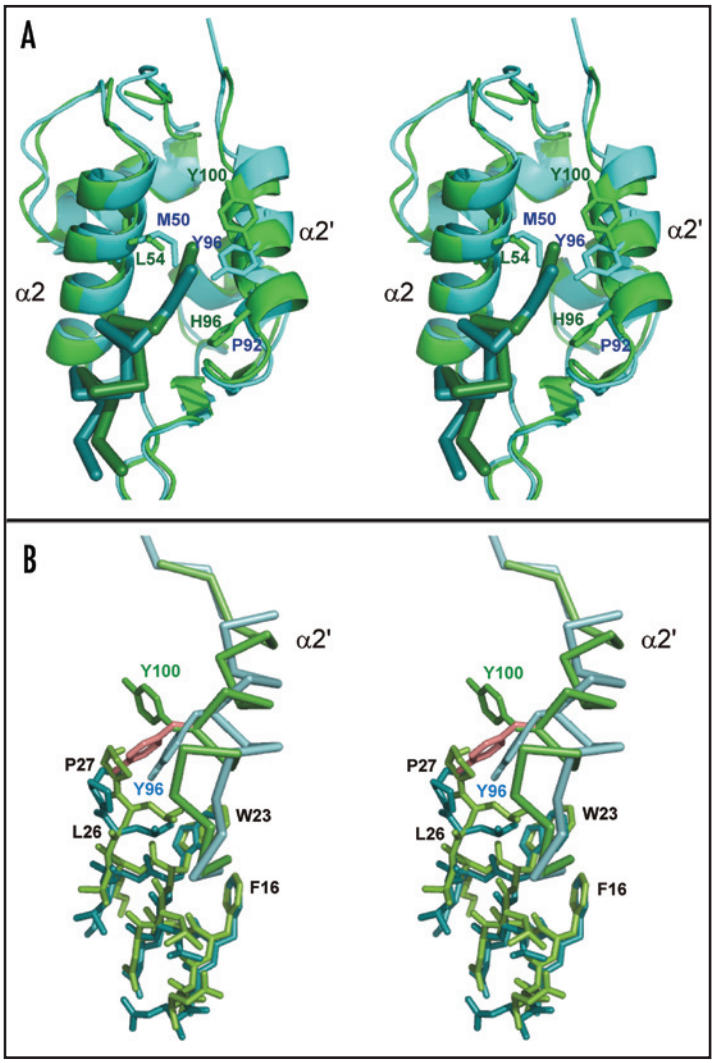

Figure 1. The structure of the complex between the variant of Mdmx (residues 15–129, mutations L46V and V95L) and p53 superimposed on the structure of the Hdm2/p53 complex. (A) Stereoview of an overlay of Mdmx (blue) and Hdm2 (green). Residues shown, M50, P92 and Y96 for zebrafish Mdmx, and L54, H96 and Y100 for Hdm2, are important for binding to p53. (B) The interaction of the p53 peptide 1 (stick plot) with α2´ helix (α-carbon plot) of Mdmx (blue) and Hdm2 (green). Tyr100 of Hdm2 in the structure of the nutlin/Hdm2 complex (26) is shown, in addition, in red.

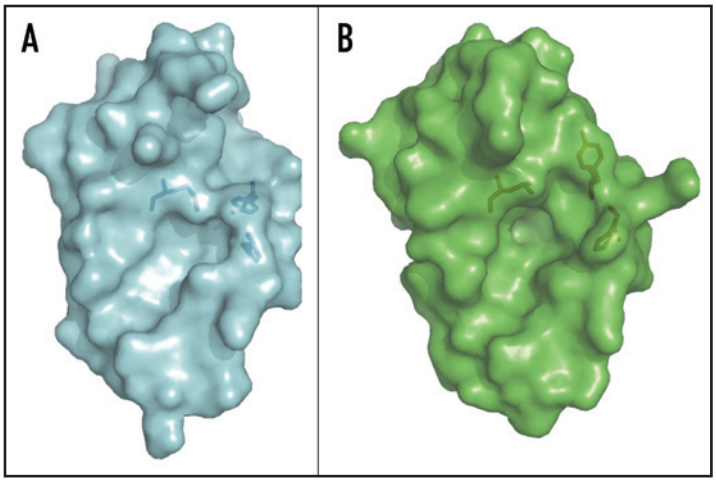

Figure 2. Surface representations of Mdmx (the left side) and Hdm2 structures (the right side). Residues highlighted are Met50, Tyr96, and Pro92 of Mdmx, and Leu54, His96, and Tyr100 of Hdm2 (see text).

and Hdmx/p53 complexes. For Hdm2, the Trp23 peak reappears on addition of nutlin-3, indicating that p53 has been fully released (Fig. 4A, lower trace). The NMR spectrum additionally showed that the freed p53 is folded, that the Hdm2/nutlin-3 complex is soluble, and that nutlin-3 did not induce precipitation of Hdm2. Nutlin-3 was however not able to efficiently disrupt the Hdmx-p53 binding at the molar ratio of the compound to protein 6:1 (Fig. 4B); even at the molar ratio 50:1 only 20% of p53 is released (data not shown). Similar results (Fig. 4C and D; Suppl. Fig. 3) were obtained for small molecular weight antagonists of Hdm2/p53 compounds called NXN-6 and NXN-7 (see ref. 47).

The structures of Mdmx´s show that, compared to Mdm2, a part of the p53 binding cleft is blocked by sidechains of Met and Tyr of Mdmx. Since these differences are relevant to nutlin binding, we have mutated these residues in Hdmx to those with smaller sidechains (mutants Met53Val and Tyr99Thr) and determined their binding to nutlin and p53 (Fig. 4E and F; Table 2). Mutation of Met53Val had a pronounced effect on dissociation capability of nutlin-3: about 40% of p53 is released; for the Tyr99Thr mutant the difference to the wt-Mdmx was not significant. This trend is in agreement with the K_D data for the direct interactions of these Hdmx mutants with p53 or nutlin-3 (Table 2). For example, the binding of nutlin-3 to mutant Met53Val is 40-fold stronger (K_D, 5 μM) than to the Tyr99Thr mutant (K_D, 200 μM) and 5-fold stronger than to wt-Hdmx ($K_{D,}$ 25 μM).

DISCUSSION

Implications for understanding of the interaction of the known Mdm2-antagonists with Mdmx. The structure of zebrafish Mdmx, in conjunction with affinity data, reveals the mechanism of p53 inhibition by Mdmx and shows why specific inhibitors of Hdm2 would only weakly bind to Mdmx. For nutlin-3, the chlorophenyl ring of nutlin-3 cannot establish a deep hydrophobic interaction with Mdmx seen in the nutlin-3/Hdm2 structure (Fig. 1B, 2 and 3). The corresponding part of the Mdmx pocket is shallow compared to that of Hdm2. Two residues of Mdmx, Met50 and Tyr96, are crucially responsible for this feature of the Mdmx cleft. The chlorine atom of nutlin-3 would be only 1.6 Å away from the OH atom of the Mdmx Tyr96 (Fig. 3). Flipping the Tyr96 aromatic ring away from the side of the p53 binding pocket would release this obstruction, but it would then lower the hydrophobicity of this side of the pocket. In addition, the flipped aromatic ring would clash with the side chain of Glu20. Figures 1B and 3 show the position of the Tyr100 aromat in the nutlin-3/Hdm2 complex (magenta) and in the p53/Hdm2 complex (green). One can see that nutlin crucially relies on establishing a hydrophobic interaction between its chlorophenyl and the aromat of Tyr100, pulling the Tyr100 ring towards the p53 interacting cleft of Hdm2 (we designate this conformation of the Tyr as the "closed conformation"). Our competition experiments for mutant Hdmx´s beautifully support this conclusion (Fig. 4): Mutation of the Hdmx-corresponding Tyr99 to Thr in Hmdx does not help the nutlin in its effectiveness to dissociate the Hdmx-p53 complex (Fig. 4B and E). However, mutation of Met53 to Val, e.g., mutating to a smaller sidechain amino acid with however uncompromised hydrophobicity, increased 2-fold the dissociating power of nutlin-3 compared to that of wt-Hdmx (Fig. 4B and F).

The PDB Data Bank contains four additional structures of complexes of Hdm2 with peptidic antagonists: 1T4F (see ref. 33), 2GV2 (see ref. 48), 2AXI (see ref. 49) and with a benzodiazepinedione

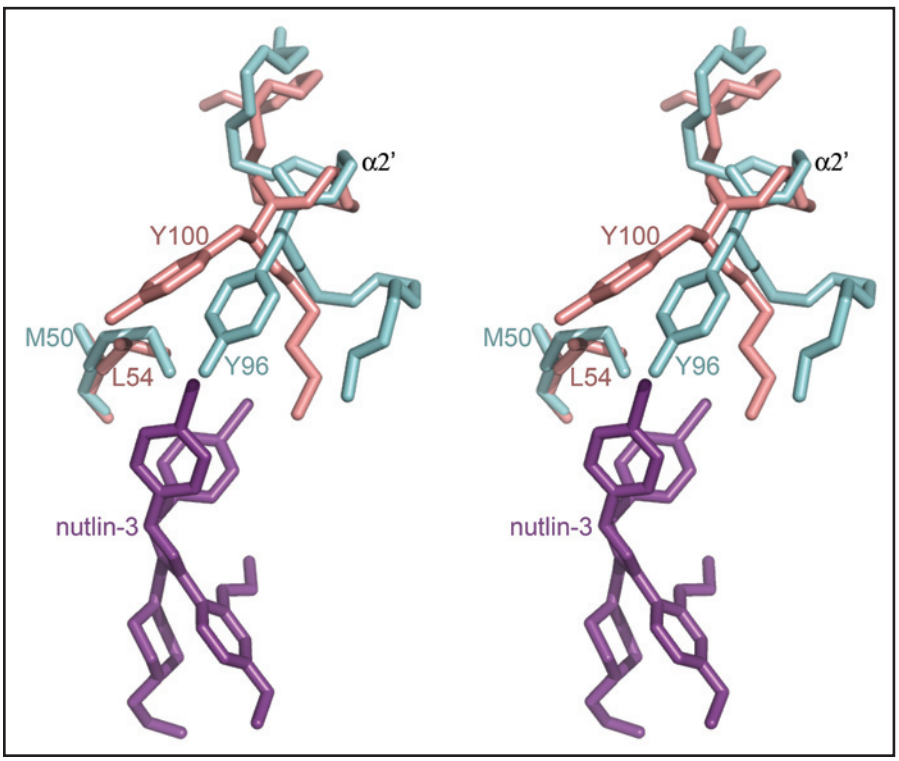

Figure 3. The interaction of nutlin-3 (stick plot) with a part of the α2´ helix (α-carbon plot) of Mdmx (blue) and Hdm2 (magenta). Tyr100 of Hdm2 in the structure of the nutlin/Hdm2 complex is shown, together with the Tyr96 of the Mdmx/p53 complex.

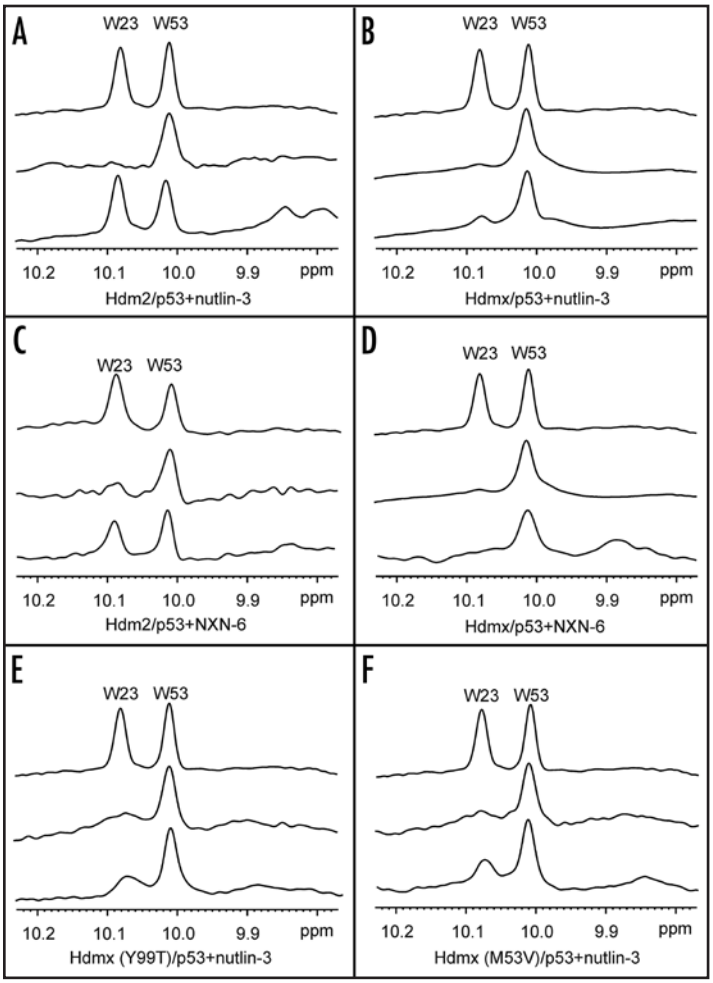

Figure 4. NMR competition binding experiments. Top spectra: 1D proton spectra of the side chains of tryptophans (W) of free p53 (residues 1–73), showing W23, W53. Middle spectra: on forming a complex with Hdm2 or Hdmx, the signal of the sidechain of W23 disappears. Bottom spectra: when we added nutlin-3, the signal of W23 recovered as a result of a complete [(A), complex Hdm2/p53] or partial dissociation of the complexes. The recovery of the W23 signal is about 15% for the Hdmx/p53 complex (B). When we added NXN-6, the signal of W23 in spectrum (C) recovered as a result of a 70% dissociation of the Hdm2/p53 complex; (D) there is a 10% recovery of the W23 signal for the Hdmx/p53 complex. The recovery of the W23 signal is about 20% for the Hdmx(Y99T)/p53 complex (E) and 45% for Hdmx(M53V)/p53 (F). The molar ratio of the compound to protein was 6:1 in all six cases.

compound (1T4E, see ref. 33). The mode of interaction between these antagonists and Hdm2 is very similar to that of the nutlin/Hdm2 structure discussed above. In all these cases Tyr100 assumes "a closed conformation" seen in the nutlin-3/Hdm2 complex. We therefore expect that the conclusions drawn here should be valid for all Mdm2/p53 antagonists reported in the literature until now. For the nutlin-like compounds, the structure of Mdmx presented here suggests a possible modification that should increase the binding: Substituting the chlorophenyl ring with a smaller, but still strongly hydrophobic group should give a scaffold more compatible with the Mdmx binding site.

Efficient inhibition of Mdmx-p53 interaction requires Mdmx targeted inhibitors. There is a controversy in the literature regarding the capability of nutlin-3 to antagonize the Mdmx-p53 interaction. Three reports saw no effect of nutlin on the Mdmx-p53 interaction,[22,25,26] whereas Laurie et al.[3,23] reported that, even though nutlin-3 binds less efficiently to Mdmx than to Mdm2, intraocular concentrations of nutlin-3 achieved by subconjunctival injection should be sufficient to disrupt both Mdm2-p53 and Mdmx-p53 in retinoblastomas.[3,23] Since the assays reported in the literature are all based on inhomogenous protein preparations, we decided to use homogenously purified proteins and check for Mdm2/x-p53 or Mdm2/x-p53/nutlin associations using direct in vitro experiments. In our approach, we primarily rely on an NMR assay that we have developed for a thorough characterization of inhibitory propensities of antagonists in protein-protein interactions.[4,39] We can thus unambiguously characterize the intrinsic properties of the interactions between Mdm2-p53 and Mdmx-p53 sequences on the molecular level. Our experiments do not capture contributions from other, secondary interacting regions of the respective proteins that might have contributed to some of the differences in the literature. However, since full-length proteins exhibit higher binding affinities in Mdmx/p53 or Mdm2/p53 complexes than the fragments (for example, the binding of Hdm2 (residues 1–118) to full-length p53 is tenfold stronger than the binding to the N-terminal domain p53 (residues 1–93); see ref. 45), it is unlikely that nutlins, which do not dissociate efficiently the complex between the N-terminal domain of Mdmx and p53 peptides, would show efficacy for the tighter bound Mdmx/p53 complexes in vitro or in vivo situations.

Our NMR and ITC binding data clearly show that Mdm2/p53 antagonists are not effective in the inhibition of the Mdmx/p53 interaction. The retinoblastoma tumor cell killing effect of nutlin-3 observed by Laurie et al.[23] could only be explained by their use of extermely high, "rancid" concentrations of nutlin-3 to block the Hdmx-p53 interaction. Nutlin-3 might also exert its action indirectly, effecting Hdmx protein levels[5] or by activating E2F1 (see refs. 50 and 51).

In conclusion, the structures of p53/Mdmx indicate that although Mdmx and Mdm2 utilize the same **p53-binding motif and many** of the same residues for binding to p53, their binding details differ significantly and thus the development of specific Hdmx inhibitors will have to take into account the unique structural properties of Hdmx. The data further suggests that there is high probability that a good binder to Hdmx would bind even stronger to Hdm2, whereas the reverse would not be true. Nutlin-3 shows this trend and we have tested several other compounds for Hdm2, all showing the same characteristcs. For example, recently developed inhibitors of the Hdm2-p53 interaction, compounds called NXN-6 and NXN-7, bind to Hdm2 with K_D's of ca. 2–5 μM, are moderately potent in dissociating the Hdm2-p53 complex, but marginally effective in antagonizing the Hdmx-p53 interaction (Fig. 4C and D). Thus, the development of new therapeutic antagonists for the Hdm2/Hdmx system should start with the screening of Hdmx first. It appears therefore that possible anti-cancer therapy based on releasing native p53 from Hdm2/Hdmx will require either mutual use of selective Hdmx and Hdm2 inhibitors or potent Hdmx antagonists, which, based on our data, are expected to also be effective in the interactions with Hdm2.

References

1. Vogelstein B, Lane D, Levine AJ. Surfing the p53 network. Nature 2000; 408:307-10.
2. Toledo F, Wahl M. Regulating the p53 pathway: In vitro hypotheses, in vivo veritas. Nat Rev Canc 2006; 6:909-23.
3. Marine JCW, Dyer MA, Jochemsen AG. MDMX: From bench to bedside. J Cell Sci 2007; 120:371-78.
4. Chene P. Inhibiting the p53-MDM2 interaction: An important target for cancer therapy. Nat Rev Cancer 2003; 3:102-9.
5. Vassilev LT. MDM2 inhibitors for cancer therapy. Trends Mol Med 2006; 13:23-31.
6. Vousden KH, Lane DP. p53 in health and disease. Nature Rev Mol Cell Biol 2007; 8:275-83.
7. Stommel JM, Wahl GM. A new twist in the feedback loop: Stress-activated MDM2 destabilization is required for p53 activation. Cell Cycle 2005; 4:411-7.
8. Meulmeester E, Pereg Y, Shiloh Y, Jochemsen AG. ATM-mediated phosphorylations inhibit Mdmx/Mdm2 stabilization by HAUSP in favor of p53 activation. Cell Cycle 2005; 4:1166-70.
9. Haupt Y, Maya R, Kazaz A, Oren M. Mdm2 promotes the rapid degradation of p53. Nature 1997; 387:296-99.
10. Kubbutat MH, Jones SN, Vousden KH. Regulation of p53 stability by Mdm2. Nature 1997; 387:299-303.
11. Momand J, Zambetti GP, Olson DC, George D, Levine AJ. The *mdm-2* oncogene product forms a complex with the p53 protein and inhibits p53-mediated transactivation. Cell 1992; 69:1237-45.
12. Ringshausen I, O'Shea CC, Finch AJ, Swigart LB, Evan GI. Mdm2 is critically and continuously required to suppress lethal p53 activity in vivo. Cancer Cell 2006; 10:501-14.
13. Oliner JD, Pietenpol JA, Thiagalingam S, Gyuris J, Kinzler KW, Vogelstein B. Oncoprotein MDM2 conceals the activation domain of tumour suppressor p53. Nature 1993; 362:857-60.
14. Lin J, Chen J, Elenbaas B, Levine AJ. Several hydrophobic amino acids in the p53 amino-terminal domain are required for transcriptional activation, binding to mdm-2 and the adenovirus 5 E1B 55-kD protein. Genes Dev 1994; 8:1235-46.
15. Picksley SM, Vojtesek B, Sparks A, Lane DP. Immunochemical analysis of the interaction of p53 with MDM2;-fine mapping of the MDM2 binding site on p53 using synthetic peptides. Oncogene 1994; 9:2523-29.
16. Kussie PH, Gorina S, Marechal V, Elenbaas B, Moreau J, Levine AJ, Pavletich NP. Structure of the MDM2 oncoprotein bound tho the p53 tumor supressor transcativation domain. Science 1996; 274:948-53.
17. Schon O, Friedler A, Bycroft M, Freund SMV, Fersht AR. Molecular mechanism of the interaction between MDM2 and p53. J Mol Biol 2002; 323:491-501.
18. Yu GW, Rudiger S, Veprintsev D, Freund S, Fernandez-Fernandez MR, Fersht AR. The central region of HDM2 provides a second binding site for p53. Proc Natl Acad Sci USA 2006; 103:1227-32.
19. Marine JC, Francoz S, Maetens M, Wahl G, Toledo F, Lozano G. Keeping p53 in check: Essential and synergistic functions of Mdm2 and Mdm4. Cell Death Differ 2006; 13:927-34.
20. Shvarts A, Steegenga WT, Riteco N, van Laar T, Dekker P, Bazuine M, van Ham RC, van der Houven van Oordt W, Hateboer G, van der Eb AJ, Jochemsen AG. MDMX: A novel p53-binding protein with some functional properties of MDM2. EMBO J 1996; 15:5349-57.
21. Francoz S, Froment P, Bogaerts S, De Clercq S, Maetens M, Doumont G, Bellefroid E, Marine JC. Mdm4 and Mdm2 cooperate to inhibit p53 activity in proliferating and quiescent cells in vivo. Proc Natl Acad Sci USA 2006; 103:3232-37.
22. Hu B, Gilkes DM, Farooqi B, Sebti SM, Chen J. MDMX overexpression prevents p53 activation by the MDM2 inhibitor Nutlin. J Biol Chem 2006; 281:33030-35.
23. Laurie NA, Donovan SL, Shih CS, Zhang J, Mills N, Fuller C, Teunisse A, Lam S, Ramos Y, Mohan A, Johnson D, Wilson M, Rodriguez-Galindo C, Quarto M, Francoz S, Mendrysa SM, Guy RK, Marine JC, Jochemsen AG, Dyer MA. Inactivation of the p53 pathway in retinoblastoma. Nature 2006; 444:61-6.
24. Toledo F, Krummel KA, Lee CJ, Liu CW, Rodewald LW, Tang M, Wahl GM. A mouse p53 mutant lacking the proline-rich domain rescues Mdm4 deficiency and provides insight into the Mdm2-Mdm4-p53 regulatory network. Cancer Cell 2006; 9:273-85.
25. Wade M, Wong ET, Tang M, Stommel JM, Wahl GM. Hdmx modulates the outcome of p53 activation in human tumor cells. J Biol Chem 2006; 281:33036-44.
26. Patton JT, Mayo LD, Singhi AD, Gudkov AV, Stark GR, Jackson MW. Levels of HdmX expression dictate the sensitivity of normal and transformed cells to Nutlin-3. Cancer Res 2006; 66:3169-76.
27. Gilkes DM, Chen J. Distinct roles of MDMX in the regulation of p53 response to ribosomal stress. Cell Cycle 2007; 6:151-5.
28. Ghosh M, Weghorst K, Berberich SJ. MdmX inhibits ARF mediated Mdm2 sumoylation. Cell Cycle 2005; 4:604-8.
29. Martins CP, Brown-Swigart L, Evan GI. Modeling the therapeutic efficacy of p53 restoration in tumors. Cell 2006; 127:1323-34.
30. Xue W, Zender L, Miething C, Dickins RA, Hernando E, Krizhanovsky V, Cordon-Cardo C, Lowe SW. Senescence and tumour clearance is triggered by p53 restoration in murine liver carcinomas. Nature 2007; 44:656-60.
31. Ventura A, Kirsch DG, McLaughlin ME, Tuveson DA, Grimm J, Lintault L, Newman J, Reczek EE, Weissleder R, Jacks T. Restoration of p53 function leads to tumour regression in vivo. Nature 2007; 445:661-65.
32. Vassilev LT, Vu BT, Graves B, Carvajal D, Podlaski F, Filipovic Z, Kong N, Kammlott U, Lukacs C, Klein C, Fotouhi N, Liu EA. In vivo activation of the p53 pathway by small-molecule antagonists of MDM2. Science 2004; 303:844-848.
33. Grasberger BL, Lu T, Schubert C, Parks DJ, Carver TE, Koblish HK, Cummings MD, LaFrance LV, Milkiewicz KL, Calvo RR, Maguire D, Lattanze J, Franks CF, Zhao S, Ramachandren K, Bylebyl GR, Zhang M, Manthey CL, Petrella EC, Pantoliano MW, Deckman IC, Spurlino JC, Maroney AC, Tomczuk BE, Molloy CJ, Bone RF. Discovery and cocrystal structure of benzodiazepinedione HDM2 antagonists that activate p53 in cells. J Med Chem 2005; 48:909-912.
34. Stoll R, Renner C, Hansen S, Palme S, Klein C, Belling A, Zeslawski W, Kamionka M, Rehm T, Muhlhahn P, Schumacher R, Hesse F, Kaluza B, Voelter W, Engh RA, Holak TA. Chalcone derivatives antagonize interactions between the human oncoprotein MDM2 and p53. Biochemistry 2001; 40:336-44.
35. Kabsch W. Automatic processing of rotation diffraction data from crystals of initially unknown symmetry and cell constants. J Appl Cryst 19934; 26:795-800.
36. CCP4, Collaborative computational project, Number 4. Acta Crystallogr Sect D 1994; 50:760-763.
37. McRee DE. XtalView/Xfit - A versatile program for manipulating atomic coordinates and electron density. J Struc Biol 1999; 125:156-65.
38. Lamzin VS, Wilson KS. Automated refinement of protein models. Acta Crystallogr Sect D 1993; 49:129-49.
39. D'Silva L, Ozdowy P, Krajewski M, Rothweiler U, Singh M, Holak TA. Monitoring the effects of antagonists on protein-protein interactions with NMR spectroscopy. J Am Chem Soc 2005; 127:13220-26.
40. Krajewski M, Ozdowy P, D'Silva L, Rothweiler U, Holak TA. NMR indicates that the small molecule RITA does not block p53-MDM2 binding in vitro. Nat Med 2005; 11:1135-36.
41. Böttger A, Böttger V, Garcia Echeverria C, Chene P, Hochkeppel HK, Sampson W, Ang K, Howard SF, Picksley SM, Lane DP. Molecular characterization of the hdm2-p53 interaction. J Mol Biol 1997; 269:744-56.
42. Böttger V, Böttger A, Howard SF, Picksley SM, Chene P, Garcia Echeverria C, Hochkeppel HK, Lane DP. Identification of novel Mdm2 binding peptides by phage display. Oncogene 1996; 13:2141-47.
43. Böttger A, Böttger V, Sparks A, Liu WL, Howard SF, Lane DP. Design of a synthetic Mdm2-binding mini protein that activates the p53 response in vivo. Curr Biol 1997; 7:860-9.
44. Böttger V, Böttger A, Garcia-Echeverria C, Ramos YF, van der Eb AJ, Jochemsen AG, Lane DP. Comparative study of the p53-mdm2 and p53-MDMX interfaces. Oncogene 1999; 18:189-99.
45. Dawson R, Mueller L, Dehner A, Klein C, Kessler H, Buchner J. The N-terminal domain of p53 is natively unfolded. J Mol Biol 2003; 332:1131-41.
46 Schon O, Friedler A, Freund S, Fersht AR. Binding of p53-derived ligands to MDM2 induces a variety of long range conformational changes. J Mol Biol 2004; 336:197-202.
47. Weber L. Tetrahydro-isoquinolin-1-ones for the treatment of cancer. International Patent 2006, (PCT/EP2006/002471).
48. Sakurai K, Schubert C, Kahne D. Crystallographic analysis of an 8-mer p53 peptide analogue complexed with MDM2. J Am Chem Soc 2006; 128:11000-1.
49. Fasan R, Dias RL, Moehle K, Zerbe O, Obrecht D, Mittl PR, Robinson JA. Structure-activity studies in a family of beta-hairpin protein epitope mimetic inhibitors of the p53-HDM2 protein-protein interaction. Chembiochem 2006; 7:515-526.
50. Ambrosini G, Sambol EB, Carvajal D, Vassilev LT, Singer S, Schwartz GK. Mouse double minute antagonist Nutlin-3a enhances chemotherapy-induced apoptosis in cancer cells with mutant p53 by activating *E2F1*. Oncogene 2007; 26:3473-81.
51. Wunderlich M, Ghosh M, Weghorst K, Berberich SJ. MdmX represses E2F1 transactivation. Cell Cycle 2004; 3:472-8.